

# Differentially Private Mixed-Type Data Generation For Unsupervised Learning

Uthaipon Tao Tantipongpipat<sup>†</sup>   Chris Waites<sup>†</sup>   Digvijay Boob  
 Amaresh Ankit Siva   Rachel Cummings\*

May 1, 2022

## Abstract

In this work we introduce the DP-auto-GAN framework for synthetic data generation, which combines the low dimensional representation of autoencoders with the flexibility of Generative Adversarial Networks (GANs). This framework can be used to take in raw sensitive data, and privately train a model for generating synthetic data that will satisfy the same statistical properties as the original data. This learned model can be used to generate arbitrary amounts of publicly available synthetic data, which can then be freely shared due to the post-processing guarantees of differential privacy. Our framework is applicable to unlabeled *mixed-type data*, that may include binary, categorical, and real-valued data. We implement this framework on both unlabeled binary data (MIMIC-III) and unlabeled mixed-type data (ADULT). We also introduce new metrics for evaluating the quality of synthetic mixed-type data, particularly in unsupervised settings.

## 1 Introduction

As data storage and analysis are becoming more cost effective, and data become more complex and unstructured, there is a growing need for sharing large datasets for research and learning purposes. This is in stark contrast to the previous statistical model where a data curator would hold datasets and answer queries from (potentially external) analysts. Sharing entire datasets allows analysts the freedom to perform their analyses in-house with their own devices and toolkits, without having to pre-specify the analyses they wish to perform. However, datasets are often proprietary or sensitive, and cannot be shared directly. This motivates the need for *synthetic data generation*, where a new dataset is created that shares the same statistical properties as the original data. These data may not be of a single type: all binary, all categorical, or all real-valued; instead they may be of *mixed-types*, containing data of multiple types in a single dataset. These data may also be unlabeled, requiring techniques for *unsupervised learning*, which is typically a more challenging task than supervised learning on labeled data.

Privacy challenges naturally arise when sharing highly sensitive datasets about individuals. Ad hoc anonymization techniques have repeatedly led to severe privacy violations when sharing “anonymized” datasets. Notable examples include the Netflix Challenge [37], the AOL Search Logs [6], and Massachusetts State Health data [40], where linkage attacks to publicly available auxiliary datasets were used to reidentify individuals in the dataset. Even deep learning model have been shown to inadvertently memoize sensitive personal information such as Social Security Numbers during training [9].

Differential privacy (DP) [16] (formally defined in Section 2) has become the de facto gold standard of privacy in the computer science literature. Informally, it bounds the amount the extent to which an

<sup>†</sup>Equal contribution

\*Georgia Institute of Technology. Email: {tao,cwaites3,digvijaybb40,ankit.siva,rachelc}@gatech.edu. U.T. supported in part by NSF grants AF-1910423 and AF-1717947. C.W. supported in part by a President’s Undergraduate Research Award from the Georgia Institute of Technology. D.B. supported in part by NSF grant CCF-1909298. R.C. supported in part by a Mozilla Research Grant, a Google Research Fellowship, and NSF grant CNS-1850187. Part of this work was completed while R.C. was visiting the Simons Institute for the Theory of Computing.

algorithm can depend on a single datapoint in its training set. This guarantee ensures that any differentially privately learned models do not overfit to individuals in the database, and therefore cannot reveal sensitive information about individuals. It is an information theoretic notion that does not rely on any assumptions of an adversary’s computational power or auxiliary knowledge. Furthermore, it has been shown empirically that training machine learning models with differential privacy protects against membership inference and model inversion attacks [50, 9]. Differentially private algorithms have been deployed at large scale in practice by organizations such as Apple, Google, Microsoft, Uber, and the U.S. Census Bureau.

Much of the prior work on differentially private synthetic data generation has been either theoretical algorithms for highly structured classes of queries [8, 24] or based on deep generative models such as Generative Adversarial Networks (GANs) or autoencoders. These architectures have been primarily designed for either all-binary or all-real-valued datasets, and have focused on the *supervised* setting, where datapoints are labelled.

In this work we introduce the *DP-auto-GAN framework*, which combines the low dimensional representation of autoencoders with the flexibility of GANs. This framework can be used to take in raw sensitive data, and privately train a model for generating synthetic data that should satisfy the same statistical properties as the original data. This learned model can be used to generate arbitrary amounts of publicly available synthetic data, which can then be freely shared due to the post-processing guarantees of differential privacy. We implement this framework on both unlabeled binary data (for comparison with previous work) and unlabeled mixed-type data. We also introduce new metrics for evaluating the quality of synthetic mixed-type data, particularly in unsupervised settings, and empirically evaluate the performance our algorithm according to these metrics on two datasets.

## 1.1 Our Contributions

In this work, we provide three main contributions: a new algorithmic framework for privately generating synthetic data, new evaluation metrics for measuring the quality of synthetic data in unsupervised settings, and empirical evaluations of our algorithmic framework using our new metrics, as well as standard metrics.

**Algorithmic Framework.** We propose a new data generation architecture which combines the versatility of an autoencoder [29] with the recent success of GANs on complex data. Our model extends previous autoencoder-based DP data generation [2, 12] by removing an assumption that the distribution of the latent space follows a mixture of Gaussian distribution. Instead, we incorporate GANs into the autoencoder framework so that the generator must learn the true latent distribution against the discriminator. We describe the composition analysis of differential privacy when the training consists of optimizing both autoencoders and GANs (with different noise parameters). Furthermore, in this analysis we halve the noise injected into autoencoder from all existing works while provably maintaining the same mathematical privacy guarantee.

**Unsupervised-Learning Evaluation Metric of Synthetic Data.** We define several new metrics that evaluate the performance of synthetic data compared to the original data when the data is of *mixed-type*. Previous metrics in the literature are applicable only to all-binary or all-real-valued datasets. Our new metrics generalize the previously used metrics [13, 55] from all-binary data to mixed-type by training various learning models to predict each feature from the rest of the data in order to assess correlation between features. In addition, our metrics do not require a particular feature to be specified as a label, and therefore do not assume a supervised-learning nature of the data, as in much of the previous work does [41, 42, 28].

**Empirical Results.** We empirically compare the performance of our algorithmic framework on the MIMIC-III medical dataset [27] and UCI ADULT Census dataset [14] using previously studied metrics in literature [18, 55]. Our experiments show that our algorithms perform better, and allow significantly improved  $\epsilon$  values with  $\epsilon \approx 1$ , compared to prior work [55] with  $\epsilon \approx 200$ . We evaluate our synthetic data using new quantitative and qualitative metrics, confirming that the performance of our algorithm remains high even for small values of  $\epsilon$ , corresponding to strong privacy guarantees. Our code is made publicly available for future use and research.

## 1.2 Related Work on Differentially Private Data Generation

Early work on differentially private synthetic data generation was focused primarily on theoretical algorithms for solving the *query release problem* of privately and accurately answering a large class of pre-specified queries on a given database. It was discovered that generating synthetic data on which the queries could be evaluated allowed for better privacy composition than simply answering all the queries directly [8, 24, 25, 19]. Bayesian inference has also been used for differentially private data generation [57, 44] by estimating the correlation between features. See Surendra & Mohan [47] for a survey of techniques used in private synthetic data generation through 2016.

In 2016, Abadi et al. [1] introduced a framework for training deep learning models with differential privacy. Non-convex optimization, which is required when training deep models, can be made differentially private by adding a Gaussian noise to a clipped (norm-bounded) gradient in each training step. Abadi et al. [1] also introduced the *moment accountant* privacy analysis for private stochastic gradient descent, which provided much tighter Gaussian-based privacy composition and allowed for significant improvements in accuracy over previously used composition techniques, such as advanced composition [17]. The moment account was later defined in terms of *Renyi Differential Privacy (RDP)* [34], which is a slight variant of differential privacy designed for easy composition, particularly for differentially private stochastic gradient descent (DP-SGD). Much of the work that followed on private data generation used deep (neural-network-based) generative models to generate synthetic data, and can be broadly categorized into two types: autoencoder-based and GAN-based. Our algorithmic framework is the first to combine both DP GANs and autoencoders into one framework.

**Differentially Private Autoencoder-Based Models.** A variational autoencoder (VAE) [29] is a generative model that compresses high-dimensional data to a smaller space called *latent space*. The compression is commonly achieved through deep models and can be differentially privately trained [12, 3]. VAE makes the (often unrealistic) assumption that the *latent distribution* is Gaussian. Acs et al. [3] uses Restricted Boltzmann machine (RBM) to learn the latent Gaussian distribution, and Abay et al. [2] uses expectation maximization to learn a Gaussian mixture. Our work extends this line of work by additionally incorporating the generative model GANs which have also been shown to be successful in learning latent distributions.

**Differentially Private GANs.** GANs are a generative model proposed by Goodfellow et al. [20] that have been shown success in generating several different types of data [36, 45, 46, 26, 30, 53]. As with other deep models, GANs can be trained privately using the aforementioned private stochastic gradient descent (formally introduced in Section 2.1). See Appendix C.1 for additional related work on performance improvements for differentially private training of deep models.

Variants of DP GANs have been used for synthetic data generation, including the Wasserstein GAN (WGAN) [5, 22] and DP-WGAN [4, 50] that use a Wasserstein-distance-based loss function in training [5, 22, 4, 50]; the conditional GAN (CGAN) [35] and DP-CGAN [49] that operate in a supervised (labeled) setting and use labels as auxiliary information in training; and Private Aggregation of Teacher Ensembles (PATE) [41, 42] for the semi-supervised setting of multi-label classification when some unlabelled public data are available (or PATEGAN [28] when no public data are available). Our work focuses on unsupervised setting where data are unlabeled, and no (relevant) labeled public data are available.

These existing works in differentially private synthetic data generation are summarized in Table 1.

**Differentially Private Generation of Mixed-Type Data.** Next we describe the three most relevant recent works on privately generating synthetic data of mixed type. Abay et al. [2] consider the problem of generating mixed-type labeled data with  $k$  possible labels. Their algorithm, DP-SYN, partitions the dataset into  $k$  sets based on the labels and trains a DP autoencoder on each partition. Then a DP expectation maximization (DP-EM) algorithm of Park et al. [43] is used to learn the distribution in the latent space of encoded data of the given label-class. The main workhorse, DM-EM algorithm, is designed and analyzed for Gaussian mixture models and more general factor analysis models. Chen et al. [12] works in the same setting, but replaces the DP autoencoder and DP-EM with a DP variational autoencoder (DP-VaE). Their algorithm assumes that the mapping from real data to the Gaussian distribution can be efficiently learned by the encoder. Finally, Frigerio et al. [18] used a Wasserstein GAN (WGAN) to generate differentially private

Table 1: Algorithmic frameworks for differentially private synthetic data generation. Our new algorithmic framework (in **bold**) is the first to combine both DP GANs and autoencoders into one framework by using GANs to learn a generative model in the latent space.

Types	Algorithmic framework	
	Main architecture	Variants
Deep generative models	DPGAN [1]	PATEGAN [28] DP Wasserstein GAN [4] DP Conditional GAN [49] Gumbel-softmax for categorical data [18]
		DP-VaE [12, 3] RBM generative models in latent space [3] Mixture of Gaussian model in latent space [2]
	Autoencoder	
	<b>Autoencoder and DPGAN (ours)</b>	
Other models	SmallDB [8], PMW [24], MWEM [25], DualQuery [19], DataSynthesizer [44], PrivBayes [57]	

mixed-type synthetic data. This type of GAN uses a Wasserstein-distance-based loss function in training. Their algorithmic framework privatized the WGAN using DP-SGD, similar to the previous approaches for image datasets [58, 55]. The methodology of Frigerio et al. [18] for generating mixed-type synthetic data involved two main ingredients: changing discrete (categorical) data to binary data using one-hot encoding, and adding an output softmax layer to the WGAN generator for every discrete variable.

Our framework is distinct from these three approaches. We use a differentially private autoencoder which, unlike DP-VaE of Chen et al. [12], does not require mapping data to a Gaussian distribution. This allows us to reduce the dimension of the problem handled by the WGAN, hence escaping the issues of high-dimensionality from the one-hot encoding of Frigerio et al. [18]. We also use DP-GAN, replacing DP-EM in Abay et al. [2], for learning distributions in the latent encoded space.

**NIST Differential Privacy Synthetic Data Challenge.** The National Institute of Standards and Technology (NIST) recently hosted a challenge to find methods for privately generating synthetic mixed-type data [38], using excerpts from the Integrated Public Use Microdata Sample (IPUMS) of the 1940 U.S. Census Data as training and test datasets. Four of the winning solutions have been made publicly available with open-source code [39]. However, all of these approaches are highly tailored to the specific datasets and evaluation metrics used in the challenge, including specialized data pre-processing methods and hard-coding details of the dataset in the algorithm. As a result, they do not provide general-purpose methods for differentially private synthetic data generation, and it would be inappropriate—if not impossible—to use any of these algorithms as baseline for other datasets such as ones we consider in this paper.

**Evaluation Metrics for Synthetic Data.** Various evaluation metrics have been considered in the literature to quantify the quality of the synthetic data (see Charest [10] for a survey). The metrics can be broadly categorized into two groups: *supervised* and *unsupervised*. Supervised evaluation metrics are used when there are clear distinctions between features and labels of the dataset, e.g., for healthcare applications, a person’s disease status is a natural label. In these settings, a predictive model is typically trained on the synthetic data, and its accuracy is measured with respect to the real (test) dataset. Unsupervised evaluation metrics are used when no feature of the data can be decisively termed as a label. Recently proposed metrics include *dimension-wise probability* for binary data [13], which compares the marginal distribution of real and synthetic data on each individual feature, and *dimension-wise prediction* which measures how closely synthetic data captures relationships between features in the real data. This metric was proposed for binary data, and we extend it here to mixed-type data. Recently, NIST [38] used a 3-way marginal evaluation metric which used three random features of the real and synthetic datasets to compute the total variation

distance as a statistical score. See Appendix C.2 for more details on both categories of metrics, including Table 2 which summarizes the metrics’ applicability to various data types.

## 2 Preliminaries on Differential Privacy

In the setting of differential privacy, a dataset  $X$  consists of  $m$  individuals’ sensitive information, and two datasets are neighbors if one can be obtained from the other by the addition or deletion of one datapoint. Differential privacy requires that an algorithm produce similar outputs on neighboring datasets, thus ensuring that the output does not overfit to its input dataset, and that the algorithm learns from the population but not from the individuals.

**Definition 1** (Differential privacy [16]). *For  $\epsilon, \delta > 0$ , an algorithm  $\mathcal{M}$  is  $(\epsilon, \delta)$ -differentially private if for any pair of neighboring databases  $X, X'$  and any subset  $S \subseteq \text{Range}(\mathcal{M})$ ,*

$$\Pr[\mathcal{M}(X) \in S] \leq e^\epsilon \cdot \Pr[\mathcal{M}(X') \in S] + \delta.$$

A smaller value of  $\epsilon$  implies stronger privacy guarantees (as the constraint above binds more tightly), but usually corresponds with decreased accuracy, relative to non-private algorithms or the same algorithm run with a larger value of  $\epsilon$ . Differential privacy is typically achieved by adding random noise that scales with the *sensitivity* of the computation being performed, which is the maximum change in the output value that can be caused by changing a single entry. Differential privacy has strong *composition guarantees*, meaning that the privacy parameters degrade gracefully as additional algorithms are run on the same dataset. It also has a *post-processing* guarantee, meaning that any function of a differentially private output will maintain the same privacy guarantees.

### 2.1 Differentially Private Stochastic Gradient Descent (DP-SGD)

Training deep learning models reduces to minimizing some (empirical) loss function  $f(X; \theta) := \frac{1}{m} \sum_{i=1}^m f(x_i; \theta)$  on a dataset  $X = \{x_i \in \mathbb{R}^n\}_{i=1}^m$ . Typically  $f$  is a nonconvex function, and a common method to minimize  $f$  is by iteratively performing stochastic gradient descent (SGD) on a batch  $B$  of sampled data points:

$$\begin{aligned} B &\leftarrow \text{BATCHSAMPLE}(X) \\ \theta &\leftarrow \theta - \eta \cdot \frac{1}{|B|} \sum_{i \in B} \nabla_{\theta} f(x_i, \theta) \end{aligned} \tag{1}$$

The size of  $B$  is typically fixed as a moderate number to ensure quick computation of gradient, while maintaining that  $\frac{1}{|B|} \sum_{i \in B} \nabla f(x_i, \theta)$  is a good estimate of true gradient  $\nabla_{\theta} f(X; \theta)$ .

To make SGD private, Abadi et al. [1] proposed to first clip the gradient of each sample to ensure the  $\ell_2$ -norm is at most  $C$ :

$$\text{CLIP}(x, C) := x \cdot \min(1, C/\|x\|_2).$$

Then a multivariate Gaussian noise parametrized by noise multiplier  $\psi$  is added before taking an average across the batch, leading to noisy-clipped-averaged gradient estimate  $g$ :

$$g \leftarrow \frac{1}{|B|} \left( \sum_{i \in B} \text{CLIP}(\nabla_{\theta} f(x_i, \theta), C) + \mathcal{N}(0, C^2 \psi^2 I) \right).$$

The quantity  $g$  is now private and can be used for the descent step  $\theta \leftarrow \theta - \eta \cdot g$  in place of Equation 1.

**Performance improvements.** In general, the descent step can be performed using other optimization methods—such as Adam or RMSProp—in a private manner, by replacing the gradient value with  $g$  in each step. Also, one does not need to clip the individual gradients, but can instead clip the gradient of a group of datapoints, called a *microbatch* [32]. Mathematically, the batch  $B$  is partitioned into microbatches  $B_1, \dots, B_k$  each of size  $r$ , and the gradient clipping is performed on the average of each microbatch:

$$g \leftarrow \frac{1}{k} \left( \sum_{i=1}^k \text{CLIP}(\nabla_{\theta} f(X_{B_i}, \theta), C) + \mathcal{N}(0, C^2 \psi^2 I) \right).$$

Standard DP-SGD corresponds to setting  $r = 1$ , but setting higher values of  $r$  (while holding  $|B|$  fixed) significantly decreases the runtime and reduces the accuracy, and does not impact privacy significantly for large dataset. Other clipping strategies have also been suggested. We refer the interested reader to [32] and Appendix C.1 for more details of clipping and other optimization strategies.

The improved moment accountant privacy analysis by [1] (which has been implemented in Google [21] and is widely used in practice) obtains a tighter privacy bound when data are subsampled, as in SGD. This analysis requires independently sampling each datapoint with a fixed probability  $q$  in each step. Additional details are also given in Appendix C.1.

The DP-SGD framework (Algorithm 1) is generically applicable to private non-convex optimization. In our proposed model, we use this framework to train the autoencoder and GAN.

---

**Algorithm 1** DP-SGD (one iteration step)

---

```

1: parameter input: Dataset  $X = \{x_i\}_{i=1}^m$ , deep learning model parameter  $\theta$ , learning rate  $\eta$ , loss function  $f$ , optimization method OPTIM, batch sampling rate  $q$  (for the batch expectation size  $b = qm$ ), clipping norm  $C$ , noise multiplier  $\psi$ , microbatch size  $r$ 
2: goal: differentially privately train one step of the model parametrized by  $\theta$  with OPTIM
3: procedure DP-SGD
4:   procedure SAMPLEBATCH( $X, q$ )
5:      $\mathcal{B} \leftarrow \{\}$ 
6:     for  $i = 1 \dots m$  do
7:       Add  $x_i$  to  $\mathcal{B}$  with probability  $q$ 
8:   return  $\mathcal{B}$ 
9:   Partition  $\mathcal{B}$  into  $B_1, \dots, B_k$  each of size  $r$  (ignoring the dividend)
10:   $\hat{k} \leftarrow \frac{qm}{r}$  ▷ an estimate of  $k$ 
11:   $g \leftarrow \frac{1}{\hat{k}} \left( \sum_{i=1}^{\hat{k}} \text{CLIP}(\nabla_{\theta} f(X_{B_i}, \theta), C) + \mathcal{N}(0, C^2 \psi^2 I) \right)$ 
12:   $\theta \leftarrow \text{OPTIM}(\theta, g, \eta)$ 

```

---

## 2.2 Renyi Differential Privacy Accountant

A variant notion of differential privacy, known as *Renyi Differential Privacy (RDP)* [34], is often used to analyze privacy for DP-SGD. A randomized mechanism  $\mathcal{M}$  is  $(\alpha, \epsilon)$ -RDP if for all neighboring databases  $X, X'$  that differ in at most one entry,

$$RDP(\alpha) := D_{\alpha}(\mathcal{M}(X) || \mathcal{M}(X')) \leq \epsilon,$$

where  $D_{\alpha}(P || Q) := \frac{1}{\alpha-1} \log \mathbb{E}_{x \sim X} \left( \frac{P(x)}{Q(x)} \right)^{\alpha}$  is the *Renyi divergence* or *Renyi entropy* of order  $\alpha$  between two distributions  $P$  and  $Q$ . Renyi divergence is better tailored to tightly capture the privacy loss from the Gaussian mechanism that is used in DG-SGD, and is a common analysis tool for DP-SGD literature. To compute the final  $(\epsilon, \delta)$ -differential privacy parameters from iterative runs of DP-SGD, one must first compute the subsampled Renyi Divergence, then compose privacy under RDP, and then convert the RDP guarantee into DP.

**Step 1: Subsampled Renyi Divergence.** Given sampling rate  $q$  and noise multiplier  $\psi$ , one can obtain RDP privacy parameters as a function of  $\alpha \geq 1$  for one run of DP-SGD [34]. We denote this function by  $RDP_{T=1}(\cdot)$ , which will depend on  $q$  and  $\psi$ .

**Step 2: Composition of RDP.** When DP-SGD is run iteratively, we can compose the Renyi privacy parameter across all runs using the following proposition.

**Proposition 2** ([34]). *If  $\mathcal{M}_1, \mathcal{M}_2$  respectively satisfy  $(\alpha, \epsilon_1), (\alpha, \epsilon_2)$ -RDP for  $\alpha \geq 1$ , then the composition of two mechanisms  $(\mathcal{M}_2(X), \mathcal{M}_1(X))$  satisfies  $(\alpha, \epsilon_1 + \epsilon_2)$ -RDP.*

Hence, we can compute RDP privacy parameters for  $T$  iterations of DP-SGD as  $\text{RDP-ACCOUNT}(T, q, \psi) := T \cdot \text{RDP}_{T=1}(\cdot)$ .

**Step 3: Conversion to  $(\epsilon, \delta)$ -DP.** After obtaining an expression for the overall RDP privacy parameter values, any  $(\alpha, \epsilon)$ -RDP guarantee can be converted into  $(\epsilon, \delta)$ -DP.

**Proposition 3** ([34]). *If  $\mathcal{M}$  satisfies  $(\alpha, \epsilon)$ -RDP for  $\alpha > 1$ , then for all  $\delta > 0$ ,  $\mathcal{M}$  satisfies  $(\epsilon + \frac{\log 1/\delta}{\alpha-1}, \delta)$ -DP.*

Since the  $\epsilon$  privacy parameter of RDP is also a function of  $\alpha$ , this last step involves optimizing for the  $\alpha$  that achieves smallest privacy parameter in Proposition 3.

### 3 Algorithmic Framework

The overview of our algorithmic framework DP-auto-GAN is shown in Figure 1, and the full details are given in Algorithm 2. Details of subroutines in Algorithm 2 can be found in Appendix A.

The algorithm takes in  $m$  raw data points, and *pre-processes* these points into  $m$  vectors  $x_1, \dots, x_m \in \mathbb{R}^n$  to be read by DP-auto-GAN, where usually  $n$  is very large. For example, categorical data may be pre-processed using one-hot encoding, or text may be converted into numerical values. Similarly, the output of DP-auto-GAN can be *post-processed* from  $\mathbb{R}^n$  back to the data's original form. We assume that this pre- and post-processing can be done based on public knowledge, such as possible categories for qualitative features and reasonable bounds on quantitative features, and therefore does not require privacy.

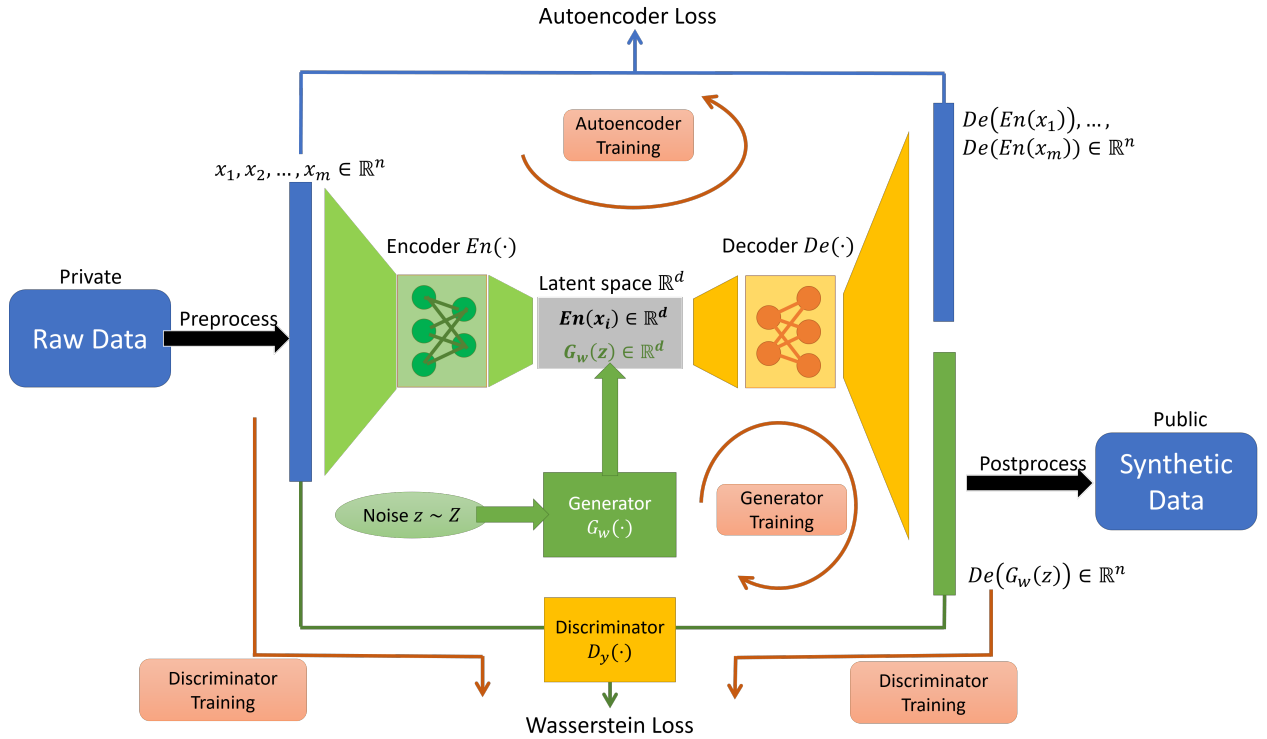


Figure 1: The summary of our DP-auto-GAN algorithmic framework. Pre- and post-processing (in black) are assumed to be public knowledge. Encoder and generator (in green) are trained without noise injection, whereas decoder and discriminator (in yellow) are trained with noise. The four red arrows indicate how data are forwarded for each training: autoencoder training, generator training, and discriminator training. After training, the generator and decoder (but not encoder) are released to the public to generate synthetic data.

Within the DP-auto-GAN, there are two main components: the *autoencoder* and the GAN. The autoencoder serves to reduce the dimensionality of the data before it is fed into the GAN. The GAN consists of a *generator* that takes in noise  $z$  sampled from distribution  $Z$  and produces  $G_w(z) \in \mathbb{R}^d$ , and a *discriminator*  $D_y(\cdot) : \mathbb{R}^n \rightarrow \{0, 1\}$ . Because of the autoencoder, the generator only needs to synthesize data based on the latent distribution  $\mathbb{R}^d$ , which is a much easier task than synthesizing in the original high-dimensional space  $\mathbb{R}^n$ . Both components of our architecture, as well as our algorithm’s overall privacy guarantee, are described in the remainder of this section.

---

**Algorithm 2** DPAUTOGAN (full procedure)

---

- 1: **architecture input:** Sensitive dataset  $D \in \mathcal{X}^m$  where  $\mathcal{X}$  is the (raw) data universe, preprocessed data dimension  $n$ , latent space dimension  $d$ , preprocessing function  $Pre : \mathcal{X} \rightarrow \mathbb{R}^n$ , post-processing function  $Post : \mathbb{R}^n \rightarrow \mathcal{X}$ , encoder architecture  $En_\phi : \mathbb{R}^n \rightarrow \mathbb{R}^d$  parameterized by  $\phi$ , decoder architecture  $De_\theta : \mathbb{R}^d \rightarrow \mathbb{R}^n$  parameterized by  $\theta$ , generator’s noise distribution  $Z$  on sample space  $\Omega(Z)$ , generator architecture  $G_w : \Omega(Z) \rightarrow \mathbb{R}^d$  parameterized by  $w$ , discriminator architecture  $D_y : \mathbb{R}^n \rightarrow \{0, 1\}$  parameterized by  $y$ .
  - 2: **autoencoder training parameters:** Learning rate  $\eta_1$ , number of iteration rounds (or optimization steps)  $T_1$ , loss function  $L_{\text{auto}}$ , optimization method  $\text{OPTIM}_{\text{auto}}$  batch sampling rate  $q_1$  (for batch expectation size  $b_1 = q_1 m$ ), clipping norm  $C_1$ , noise multiplier  $\psi_1$ , microbatch size  $r_1$
  - 3: **generator training parameters:** Learning rate  $\eta_2$ , batch size  $b_2$ , loss function  $L_G$ , optimization method  $\text{OPTIM}_G$ , number of generator iteration rounds (or optimization steps)  $T_2$
  - 4: **discriminator training parameters:** Learning rate  $\eta_3$ , number of discriminator iterations per generator step  $t_D$ , loss function  $L_D$ , optimization method  $\text{OPTIM}_D$ , batch sampling rate  $q_3$  (for batch expectation size  $b_3 = q_3 m$ ), clipping norm  $C_3$ , noise multiplier  $\psi_3$ , microbatch size  $r_3$
  - 5: **privacy parameter**  $\delta > 0$
  - 6: **procedure** DPAUTOGAN
  - 7:    $X \leftarrow Pre(D)$
  - 8:   Initialize  $\phi, \theta, w, y$  for  $En_\phi, De_\theta, G_w, D_y$   
      $\triangleright$  Phase 1: autoencoder training
  - 9:   **for**  $t = 1 \dots T_1$  **do**
  - 10:      $\text{DPTRAIN}_{\text{AUTO}}(X, En, De, \text{autoencoder training parameters})$   
      $\triangleright$  Phase 2: GAN training
  - 11:   **for**  $t = 1 \dots T_2$  **do**
  - 12:     **for**  $j = 1 \dots t_D$  **do**  $\triangleright$  (privately) train  $D_y$  for  $t_D$  iterations
  - 13:        $\text{DPTRAIN}_{\text{DISCRIMINATOR}}(X, Z, G, De, D, \text{discriminator training parameters})$
  - 14:      $\text{TRAIN}_{\text{GENERATOR}}(Z, G, De, D, \text{generator training parameters})$   
      $\triangleright$  Privacy accounting
  - 15:    $\text{RDP}_{\text{auto}}(\cdot) \leftarrow \text{RDP-ACCOUNT}(T_1, q_1, \psi_1, r_1)$
  - 16:    $\text{RDP}_D(\cdot) \leftarrow \text{RDP-ACCOUNT}(T_2 \cdot t_D, q_3, \psi_3, r_3)$
  - 17:    $\epsilon \leftarrow \text{GET-EPS}(\text{RDP}_{\text{auto}}(\cdot) + \text{RDP}_D(\cdot))$
  - 18: **return** model  $(G_w, De_\theta)$ , privacy  $(\epsilon, \delta)$
- 

### 3.1 Autoencoder Training

The autoencoder consists of the encoder  $En_\phi(\cdot) : \mathbb{R}^n \rightarrow \mathbb{R}^d$  and decoder  $De_\theta(\cdot) : \mathbb{R}^d \rightarrow \mathbb{R}^n$  parametrized by edge weights  $\phi, \theta$ , respectively. The architecture of the autoencoder assumes that high-dimensional data  $x_i \in \mathbb{R}^n$  can be represented compactly in low-dimensional space  $\mathbb{R}^d$ , also called *latent space*. The encoder  $En_\phi$  is trained to find such low-dimensional representations. We also need the decoder,  $De_\theta$ , to map this point  $En_\phi(x_i)$  in the latent space back to  $x_i$ . A measure of the information preserved in this process is the error between the decoder’s image and the original  $x_i$ . Thus a good autoencoder should minimize the distance



$\text{dist}(De_\theta(En_\phi(x_i)), x_i)$  for each datapoint  $x_i$  and the appropriate distance function  $\text{dist}$ . Our autoencoder uses binary cross entropy loss:  $\text{dist}(x, y) = -\sum_{j=1}^n y_{(j)} \log(x_{(j)}) - \sum_{j=1}^n (1 - y_{(j)}) \log(1 - x_{(j)})$  (where  $x_{(j)}$  is the  $j$ th coordinate of  $x \in \mathbb{R}^n$ ).

This also motivates a definition of a (true) loss function  $\mathbb{E}_{x \sim Z_X} [\text{dist}(De_\theta(En_\phi(x_i)), x_i)]$  when data are drawn independently from an underlying distribution  $Z_X$ . The corresponding empirical loss function when we have an access to sample  $\{x_i\}_{i=1}^m$  is

$$L_{\text{auto}}(\phi, \theta) := \sum_{i=1}^m \text{dist}(De_\theta(En_\phi(x_i)), x_i). \quad (2)$$

The task of finding a good autoencoder reduces to optimizing  $\phi$  and  $\theta$  to yield small empirical loss as in Equation 2.

We minimize Equation 2 privately using DP-SGD (described in Section 2.1). Our approach differs from previous work on private training of autoencoders [12, 3, 2] by *not* adding noise to the encoder during DP-SGD, whereas previous work adds noise to both the encoder and decoder. This improves performance by reducing the noise injected into the model by half, while still maintaining the same privacy guarantee (see Proposition 5). The full description of our autoencoder training is given in Algorithm 3 in Appendix A. In our DP-auto-GAN framework, the autoencoder is trained first until completion, and is then fixed for the second phase of training GAN.

### 3.2 GAN Training

A GAN consists of the generator  $G_w$  and discriminator  $D_y : \mathbb{R}^n \rightarrow \{0, 1\}$ , parameterized respectively by edge weights  $w$  and  $y$ . The aim of the generator  $G_w$  is to synthesize (fake) data similar to the real dataset, while the aim of discriminator is to determine whether an input  $x_i$  is from the generator’s synthesized data (and assigning label  $D_y(x_i) = 0$ ) or is real data (and assigning label  $D_y(x_i) = 1$ ). The generator is seeded with a random noise  $z \sim Z$  that contains no information about real dataset, such as a multivariate Gaussian vector, and aims to generate a distribution  $G_w(z)$  that is hard for  $D_y$  is distinguish from the real data. Hence, the generator wants to minimize the probability that  $D_y$  makes a correct guess,  $\mathbb{E}_{z \sim Z} [1 - D_y(G_w(z))]$ . At the same time, the discriminator wants to maximize its probability of correct guess when the data is fake  $\mathbb{E}_{z \sim Z} [1 - D_y(G_w(z))]$  and when the data is real  $\mathbb{E}_{x \sim Z_X} [D_y(x)]$ .

We generalize the output of  $D_y$  to a continuous range  $[0, 1]$ , with the value indicating the confidence that a sample is real. We use the zero-sum objective for the discriminator and generator proposed by Arjovsky et al. [5] and motivated by the Wasserstein distance of two distributions. Although their proposed Wasserstein objective cannot be computed exactly, it can be approximated by optimizing the objective:

$$\min_y \max_w O(y, w) := \mathbb{E}_{x \sim Z_X} [D_y(x)] - \mathbb{E}_{z \sim Z} [D_y(G_w(z))]. \quad (3)$$

We optimize Equation 3 privately using the DP-SGD framework described in Section 2.1. We differ from prior work on DP GANs in that our generator  $G_w(\cdot)$  outputs data  $G_w(z)$  in latent space  $\mathbb{R}^d$  which needs to be decoded to  $De(G_w(z))$  before being fed into the discriminator  $D_y(z)$ . The gradient  $\nabla_w G_w$  is obtained by backpropagation through one more component  $En(\cdot)$ . Hence, the training of generator remains totally private because the additional component  $En(\cdot)$  is fixed and never accesses the private data. The full description of our GAN training is given in Algorithm 5 in the Appendix A.

At the end of the two-phase training (including autoencoder and GAN), the noise distribution  $Z$ , trained generator  $G_w(\cdot)$ , and trained decoder  $De(\cdot)$  are released to the public. The public can then generate synthetic data by sampling  $z \sim Z$  to obtain a synthesized datapoint  $En(G_w(z))$  repeatedly to obtain a synthetic dataset of any desired size.

### 3.3 Privacy Accounting

Our autoencoder and GAN are trained privately by adding noise to the encoder and discriminator. Since the generator only accesses data through the discriminator’s (privatized) output, then the trained parameters of

generator are also private by post-processing guarantees of differential privacy. Finally, we release the privatized decoder and generator, together with generator’s noise distribution  $Z$  and post-processing procedure, both of which are assumed to be public knowledge.

The privacy accounting is therefore required for the two parts that access real data  $X$ : training the autoencoder and the discriminator. In each training procedure, we apply the RDP accountant described in Section 2.2 to analyze privacy of the DP-SGD training algorithm, to compute final  $(\epsilon, \delta)$ -DP bound. Our application of the RDP accountant diverges from the previous literature in two main ways.

First, we do not add noise to encoder during the autoencoder training, which is contrary to prior work that adds noise to both the encoder and decoder. Our approach of not adding noise to the encoder does not affect the algorithms’ overall privacy guarantees. This claim is stated formally in the following corollary, which follows immediately by instantiating Proposition 5 with the RDP privacy accountant and then composing RDP using Proposition 2.

**Corollary 4.** *If the decoder in DP-auto-GAN is trained privately with RDP privacy parameter  $\text{RDP}_{\text{auto}}(\cdot)$  (the encoder can be trained non-privately) and the discriminator in DP-auto-GAN is trained with RDP privacy parameter  $\text{RDP}_D(\cdot)$ , then DP-auto-GAN is RDP with privacy parameter  $\text{RDP}_{\text{auto}}(\cdot) + \text{RDP}_D(\cdot)$ .*

Second, the privacy analysis must account for two phases of training, usually with different privacy parameters (due to different batch sampling rates, noise, and number of iterations). One obvious solution is to calculate the desired  $(\epsilon, \delta)$ -DP parameter obtained from each phase and compose them to obtain  $(\epsilon_1 + \epsilon_2, \delta_1 + \delta_2)$ -DP using basic composition of differential privacy [16]. However, we can obtain a tighter privacy bound by composing the privacy at the Renyi Divergence level before translating Renyi Divergence into  $(\epsilon, \delta)$ -DP. In other words, we first apply Proposition 2 to compute  $\text{RDP}(\cdot)$  of two-phase training before applying Proposition 3 to translate RDP into DP, as analogous to the approach described in Section 2.2 for RDP composition for DP-SGD. This is the approach highlighted in Corollary 4. In practice, this reduces the privacy parameter  $\epsilon$  by about 30%.

## 4 Evaluation Metrics

In this section, we discuss the evaluation metrics that we use in the experiments (described in Section 5) to empirically measure the quality of the synthetic data. Some of these metrics have been used in the literature, while many are novel contributions in this work. The evaluation metrics are summarized in Table 2; our contributions are in bold.

For the first two metrics described below, the dataset should be partitioned into a training set  $R \in \mathbb{R}^{m_1 \times n}$  and testing set  $T \in \mathbb{R}^{m_2 \times n}$ , where  $m = m_1 + m_2$  is the total number of samples the real data, and  $n$  is the number of features in the data. After training the DP-auto-GAN, we use it to create a synthetic dataset  $S \in \mathbb{R}^{m_3 \times n}$ , for sufficiently large  $m_3$ .

**Dimension-wise probability.** This metric is used when the entire dataset is binary, and it serves as a basic sanity check to verify whether DP-auto-GAN has correctly learned the marginal distribution of each feature. Specifically, it compares the proportion of 1’s (which can be thought of as estimators of Bernoulli success probability) in each feature of the training set  $R$  and synthetic dataset  $S$ .

**Dimension-wise prediction.** This metric evaluates whether DP-auto-GAN has correctly learned the relationships *between* features. For the  $k$ -th feature of training set  $R$  and synthetic dataset  $S$ , we choose  $y_{R_k} \in \mathbb{R}^{m_1}$  and  $y_{S_k} \in \mathbb{R}^{m_3}$  as labels of a classification or regression task based on the type of that feature, and the remaining features  $R_{-k}$  and  $S_{-k}$  are used for prediction. We train either a classification or regression model and measure goodness of fit based on the model’s accuracy using the following well known metrics:

1. Area under the ROC curve (AUROC) score and  $F_1$  score for classification: The  $F_1$  score of a classifier is defined as  $F_1 := \frac{2 \times \text{precision} \times \text{recall}}{\text{precision} + \text{recall}}$ , where precision is ratio of true positives to true and false positives, and recall is ratio of true positives to total true positives (i.e., true positives plus false negatives). AUROC score is a graphical measure capturing the area under ROC (receiver operating characteristic) curve, and is only intended for binary data. Both metrics take values in interval  $[0, 1]$  with larger values implying good fit.

Table 2: Summary of evaluation metrics in DP synthetic data generation. We list applicability of each metric to each of the data type. Parts in **bold** are **our new contributions**. Evaluation methods with asterisk \* are predictive-model-specific, and their applicability therefore depends on types of data that the chosen predictive model is appropriate for. Methods with asterisks \*\* are equipped with any any distributional distance of choice such as Wasserstein distance.

TYPES	EVALUATION METHODS	DATA TYPES		
		Binary	Categorical	Regression
Supervised	Label prediction* [12, 2, 18]	Yes	Yes	Yes
	Predictive model ranking* [28]	Yes	Yes	Yes
Unsupervised, prediction-based	Dimension-wise prediction plot*	Yes ([13], <b>ours</b> )	<b>Yes</b>	<b>Yes</b>
Unsupervised, distributional-distance-based	Dimension-wise probability plot [13]	Yes	No	No
	3-way feature marginal, total variation distance [38]	Yes	Yes	Yes
	<b><math>k</math>-way feature marginal**</b>	<b>Yes</b>	<b>Yes</b>	<b>Yes</b>
	<b><math>k</math>-way PCA marginal**</b>	<b>Yes</b>	<b>Yes</b>	<b>Yes</b>
	<b>Distributional distance**</b>	<b>Yes</b>	<b>Yes</b>	<b>Yes</b>
<b>Unsupervised, qualitative</b>	1-way feature marginal (histogram)	Yes	Yes	Yes
	2-way PCA marginal (data visualization)	Yes	Yes	Yes

2.  $R^2$  score for regression: The  $R^2$  score is defined as  $1 - \frac{\sum (y_i - \hat{y}_i)^2}{\sum (y_i - \bar{y})^2}$ , where  $y_i$  is the true label,  $\hat{y}_i$  is the predicted label, and  $\bar{y}$  is the mean of the true labels. This is a popular metric used to measure goodness of fit as well as future prediction accuracy for regression.

We also propose following novel evaluation metrics.

**1-way feature marginal.** This metric works as a sanity check for real features. We compute histograms for the feature interest of both real and synthetic data. The quality of the synthetic data with respect to this metric can be evaluated qualitatively through visual comparison of the histograms on real and synthetic data. This can be extended to  $k$ -way feature marginals and made into a quantitative measure by adding a distance measure between the histograms.

**2-way PCA marginal.** This metric generalizes the 3-way marginal score used in NIST [38]. In particular, we compute principle components of the original data and evaluate a projection operator for first two principle components. Let us denote  $P \in \mathbb{R}^{n \times 2}$  as the projection matrix such that  $\bar{R} = RP$  is the projection on first two principle components of  $R$ . Then we evaluate projection of synthetic data  $\bar{S} = SP$  and scatter-plot 2-D points in  $\bar{R}$  and  $\bar{S}$  for visual evaluation. For quantitative evaluation, we also compute Wasserstein distance between  $\bar{R}$  and  $\bar{S}$ . In the simulations described in Section 5, we used Wasserstein distance since we optimize for the WGAN objective, but any distributional divergence metric can be used. This approach can also be extended to  $k$ -way marginals by making the projection matrix  $P \in \mathbb{R}^{n \times 2}$  for the first  $k$  principle components.

**Distributional distance.** In this metric, we first compute the Wasserstein distance  $W_2(R, S)$  between the entire real and synthetic datasets  $R, S$ . The Wasserstein score is then defined as

$$W_{\text{score}}(R, S) := 1 - \frac{W_2(R, S)}{\max_{x, y \in \mathcal{X}} \|x - y\|_2^2},$$

where the Wasserstein distance is normalized by the maximum distance possible of two datapoints in data

universe  $\mathcal{X}$ . To compute the Wasserstein score on  $k$ -way marginal PCA projection  $P$ , we normalize the score with additional term  $\sqrt{v}$ , where  $v$  is the explained variance of  $P$ :

$$W_{\text{score}}(\bar{R}, \bar{S}, P) := 1 - \frac{W_2(\bar{R}, \bar{S})}{\sqrt{v} \max_{x, y \in \mathcal{X}} \|x - y\|_2^2}.$$

For more details about implementation of these new evaluation metrics, their generalizations and relationships among them, we refer the reader to Appendix C.2.

## 5 Experiments

In this section we present details of our datasets and show empirical results of our experiments. Throughout our experiments, we fix  $\delta = 10^{-5}$  for training DP-auto-GAN and show results for different values of  $\epsilon$  including  $\epsilon = \infty$  (i.e., non-private GAN) which serves as a benchmark. We also compare our results with existing works in the literature where relevant. Details of hyper-parameters and architecture can be found in the appendix. The code of our implementation is available at <https://github.com/DPautoGAN/DPautoGAN>.

### 5.1 Binary Data

First, we consider the MIMIC-III dataset [27] which is a publicly available dataset consisting of medical records of 46K intensive care unit (ICU) patients over 11 years old. This is a binary dataset with 1071 features.

Even though our DP-auto-GAN framework can handle mixed-type data, we first evaluate it on the MIMIC-III dataset, which is all binary, since this dataset has been used in similar non-private [13] and private [55] GAN frameworks. We use the same evaluation metrics used in these papers. First we plot dimension-wise probability for DP-auto-GAN run on this dataset.

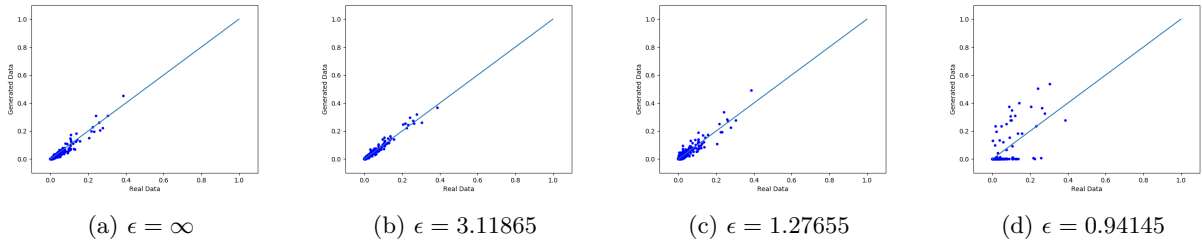


Figure 2: Dimension-wise probability scatterplots for different values of  $\epsilon$ . For each point in the plot represents one of the 1071 features in MIMIC-III dataset. The  $x$  and  $y$  coordinates of each point are the proportion of 1 in real and synthetic datasets of a feature, respectively. The line  $y = x$  is shown in each plot.

As shown in Figure 2, the proportion of 1's in the marginal distribution for is similar on the real and synthetic datasets for  $\epsilon = \infty$  and  $\epsilon = 3.11865$ , because nearly all points fall close to the line  $y = x$ . The performance of DP-auto-GAN is affected marginally for  $\epsilon = 1.27655$  which can be noticed by increased variance of points along line  $y = x$ . For  $\epsilon = 0.94145$ , DP-auto-GAN is unable to accurately learn the marginal distributions in the real data, as many of the features in the synthetic dataset have much higher proportion of 0's. This trend in the performance is expected for smaller values of  $\epsilon$ , which correspond to stronger privacy guarantees. We note that our results are significantly stronger than the ones obtained in [55] with  $\epsilon \in [96.5, 231]$  because we obtain dramatically better performance with  $\epsilon$  values that are two orders of magnitude smaller. For visual performance comparison, see Figures 4 and 5 of [55].

Figure 3 shows the plots of dimension-wise prediction using DP-auto-GAN for different values of  $\epsilon$ . As shown in the figure, for  $\epsilon = \infty$ , many points are concentrated along the lower side of line  $y = x$ , which indicates that the AUROC score of the real dataset is only marginally higher than that of the synthetic

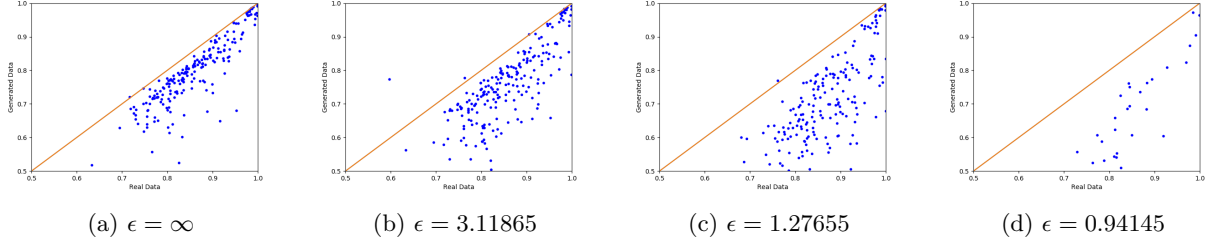


Figure 3: Dimension-wise prediction scatterplots for different values of  $\epsilon$ . Each point represents one of 1071 features in MIMIC-III dataset. For each point, the  $x$  and  $y$  coordinates represent the AUROC score of a logistic regression classifier trained on real and synthetic datasets, respectively. The line  $y = x$  corresponds to the ideal performance.

dataset. For  $\epsilon = 3.11865$  and  $\epsilon = 1.27655$ , there is a gradual shift downwards relative to the line  $y = x$ , with larger variance in the plotted points. This indicates that AUROC scores of real and synthetic data shows more difference for smaller values of  $\epsilon$ . The plot for  $\epsilon = 0.94145$  shows the same trend, but has noticeably fewer datapoints plotted. This is because many features in the synthetic data under this small  $\epsilon$  value have a high proportion of 0's, so the logistic regression classifier trained on these features uniformly outputs 0 on the hold-out test dataset  $T$ . In such cases, the AUROC score is  $1/2$  by default and as such, does not have any meaning, so we drop those features from the plot. The plots of dimension-wise prediction with these points included are given in Figure 7 in Appendix B.2, along with training specifications of DP-auto-GAN on the MIMIC-III dataset in Appendix B.1.

## 5.2 Mixed Data

Second, we consider the ADULT dataset [14] which is an extract of the U.S. Census and contains information about working adults. This dataset has 14 features out of which 10 features are categorical and four are real-valued.

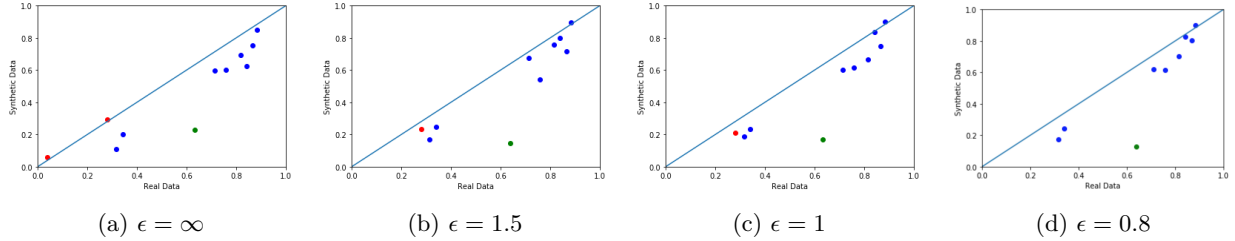


Figure 4: Dimension-wise prediction scatterplot for different values of  $\epsilon$ . Each point represents one of 14 features in the ADULT dataset. Blue points and single green points correspond to categorical features, and are plotted according to  $F_1$  score. Red points correspond to real-valued features, and we plot  $R^2$  score when it is positive. For each point,  $x$  and  $y$  coordinate represents relevant score evaluated on real and synthetic datasets, respectively.

Figure 4 shows the dimension-wise prediction plot of DP-auto-GAN on this dataset. For categorical features (represented by blue points and a single green point), we use random forest classifier in order to compare our result with [18]. For real-valued features (represented by red points), we used a lasso regression model. The green point corresponds to the *salary* feature of the data, which is real-valued but treated as binary, based on the condition  $> \$50k$ , which is similarly used as a binary label in [18]. We use  $F_1$  score as our classification accuracy measure for categorical features in in Figure 4, and we use  $R^2$  score as our regression accuracy for real-valued features. The  $F_1$  score is preferred over AUROC score for the ADULT

Table 3: Accuracy scores of prediction on salary feature evaluated on different  $\epsilon$  values.

$\epsilon$ value	Real dataset	$\infty$	7	3	1.5	1	0.8
Accuracy (ours)	86.63%	79.18%			77.86%	76.92%	77.7%
Accuracy ([18])	77.2%	76.7%	76.0%	75.3%			

dataset because it has many non-binary features where AUROC cannot be used. Each point in Figure 4 corresponds to one feature, and the  $x$  and  $y$  coordinates respectively show the accuracy score on the real data and the synthetic data.

Similar to the MIMIC-III dataset, we see that for large values of  $\epsilon$ , points are scattered close to  $y = x$  line, and as  $\epsilon$  gets smaller, points gradually shift downward implying, that accuracy of synthetic data decreases with stronger privacy guarantees. For the salary feature, we also compute accuracy scores for comparison with [18]. In Table 3, we report the accuracy of each synthetic dataset as well as benchmark accuracy. The results reported in [18] use  $\epsilon = 3, 7, \infty$ , whereas our algorithms used parameter values  $\epsilon = 0.8, 1, 1.5, \infty$ . We see that our accuracy guarantees are higher than those of [18] with smaller  $\epsilon$  values, and DP-auto-GAN achieved higher accuracy in the non-private setting.

Note that in the ADULT dataset, we have four real-valued features (age, capital gain, capital loss, and hours worked per week), but there are not four red points in each plot of Figure 4. While AUROC for the binary features is always supported on  $[0, 1]$ , the  $R^2$  score for real-valued features can be negative if the predictive model is poor, and these values fell outside the range of Figure 4. As  $\epsilon$  decreased—corresponding to stronger privacy and hence diminished accuracy of performance—fewer red points are observed in Figure 4. We were not able to find a regression model with good fit (as measured by  $R^2$  score) for the latter three features (capital gain, capital loss, and hours worked per week) in terms of the other features even on the real data. We attempted several different approaches, ranging from simple regression models such as lasso to complex models such as neural networks, and all had a low  $R^2$  score on both the real and synthetic data. The capital gain and capital loss attributes are inherently hard to predict because the data are sparse (mostly zero) in these attributes.

Since the  $R^2$  did not prove to be a good metric for these features, we instead plotted 1-way feature marginal histograms for each of these three remaining features to check whether the marginal distribution was learned correctly. These 1-way histograms are shown in Figure 5. The figure shows that DP-auto-GAN identifies the marginal distribution of capital gain and capital loss quite well, and it does reasonably well on the hours-per-week feature.

In order to understand combined performance of all features, we use two metrics. First, we show the qualitative results from 2-way PCA marginal score in Figure 6. A close qualitative inspection of plots clearly shows the similarities of trends between the plots for real dataset and for different values of  $\epsilon$ , as low as  $\epsilon = 1$ . We can turn this qualitative measure into a quantitative one by evaluating the Wasserstein distributional distance between the synthetic and real data, shown in Table 4. We measure this distance both on the 2-way PCA marginal distribution and on the full dataset. Computing exact Wasserstein distance can be computationally expensive; in practice, we uniformly sample datapoints from real and synthetic (projected) data to compute Wasserstein distance. This sampling and distance computation are repeated several times, and the average of the distances over all iterations is used as the final Wasserstein distance.

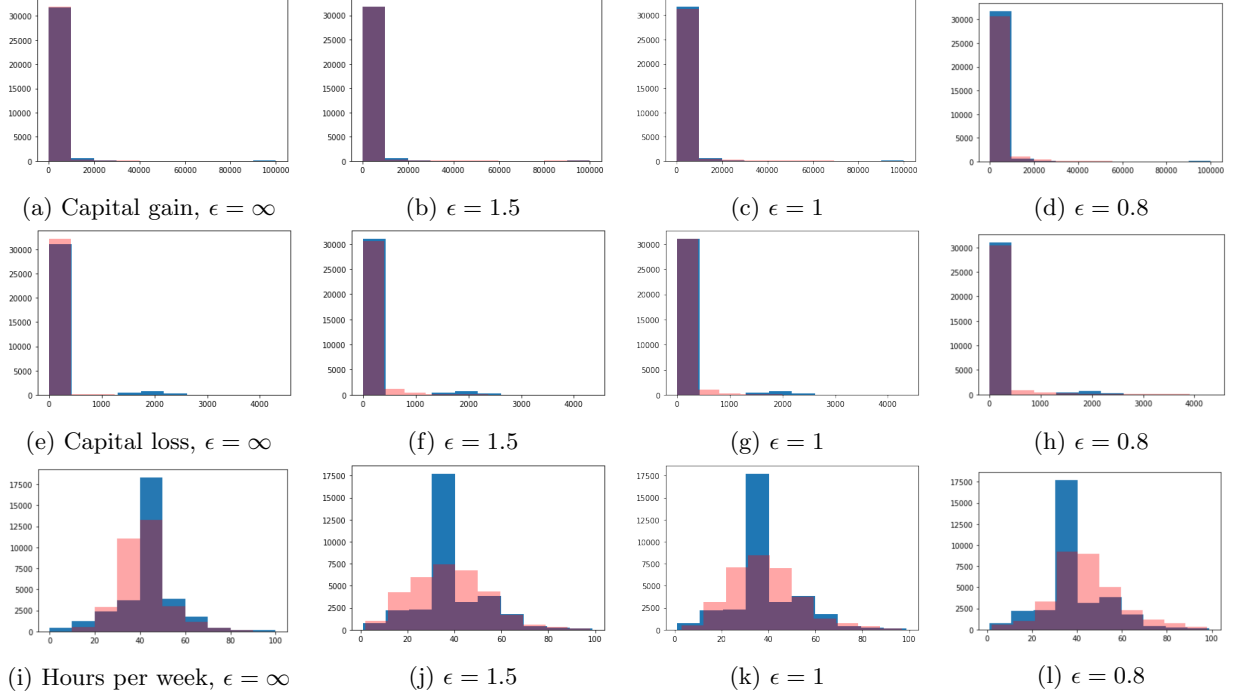


Figure 5: 1-way histogram for different values of  $\epsilon$ . Three rows correspond to capital gain, capital loss and weekly work-hours. Blue corresponds to the histogram of the real dataset, and red corresponds to the histogram of the synthetic dataset generated with the indicated  $\epsilon$ . The overlap of both histograms is purple.

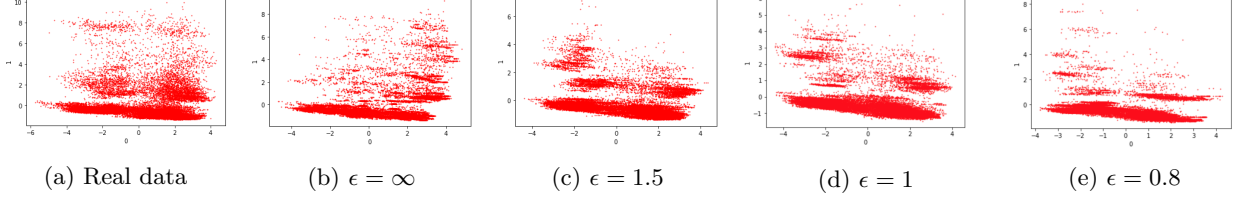


Figure 6: Scatterplot of projection of given dataset on first two principle component of the real dataset

Table 4: Wasserstein distance scores on 2-way PCA marginals and on the whole dataset for different  $\epsilon$  values.

Method	$\epsilon$	2-way PCA score	Whole-data score
DP-auto-GAN	1.5	44.36%	60.84%
DP-auto-GAN	1	41.17%	60.53%
DP-auto-GAN	0.8	19.25%	60.51%

## 6 Conclusion

We proposed a method called DP-auto-GAN for differentially private synthetic data generation. This method combines the efficient low-dimensional representation of variational autoencoders with the flexibility and versatility of GANs. Relative to prior work on differentially private autoencoders, we show that it suffices

to only train the decoder privately, which allows the noise from privacy to be reduced by a factor of 2.

We show how this framework can be used to privately learn a model for generating synthetic data, and once trained, this model can then be used to generate arbitrary amounts of synthetic data that will enjoy the same privacy guarantees, due to the post-processing property of differential privacy. This method can be used for *mixed-type data*, that includes binary, categorical, and real valued data.

We introduce a number of new metrics for evaluating the quality of mixed-type synthetic data, particularly in unsupervised settings. We then evaluate the performance of our DP-auto-GAN algorithm on two datasets (one all-binary and one mixed-type data) using our new metrics as well as existing metrics from the literature. We show that DP-auto-GAN performs better than existing techniques in terms of the privacy-accuracy tradeoff for a wide variety of accuracy metrics.

## References

- [1] Martin Abadi, Andy Chu, Ian Goodfellow, H. Brendan McMahan, Ilya Mironov, Kunal Talwar, and Li Zhang. Deep learning with differential privacy. In *Proceedings of the 2016 ACM Conference on Computer and Communications Security, CCS '16*, pp. 308–318, 2016.
- [2] Nazmiye Ceren Abay, Yan Zhou, Murat Kantarcioglu, Bhavani Thuraisingham, and Latanya Sweeney. Privacy preserving synthetic data release using deep learning. In *Machine Learning and Knowledge Discovery in Databases (ECML PKDD '18)*, volume 11051 of *Lecture Notes in Computer Science*, pp. 510–526. Springer, 2018.
- [3] Gergely Acs, Luca Melis, Claude Castelluccia, and Emiliano De Cristofaro. Differentially private mixture of generative neural networks. *IEEE Transactions on Knowledge and Data Engineering*, 31(6):1109–1121, 2018.
- [4] Moustafa Alzantot and Mani Srivastava. Differential Privacy Synthetic Data Generation using WGANs, 2019. URL <https://github.com/nesl/nist-differential-privacy-synthetic-data-challenge/>.
- [5] Martin Arjovsky, Soumith Chintala, and Léon Bottou. Wasserstein GAN. arXiv preprint 1701.07875, 2017.
- [6] Michael Barbaro and Tom Zeller. A face is exposed for AOL searcher no. 4417749, August 9 2006. URL <https://www.nytimes.com/2006/08/09/technology/09aol.html>. [Online, Retrieved 9/25/2019].
- [7] Brett K. Beaulieu-Jones, Zhiwei Steven Wu, Chris Williams, Ran Lee, Sanjeev P. Bhavnani, James Brian Byrd, and Casey S. Greene. Privacy-preserving generative deep neural networks support clinical data sharing. *Circulation: Cardiovascular Quality and Outcomes*, 12(7):e005122, 2019.
- [8] Avrim Blum, Katrina Ligett, and Aaron Roth. A learning theory approach to non-interactive database privacy. In *Proceedings of the 40th annual ACM Symposium on Theory of Computing, STOC '08*, pp. 609–618, 2008.
- [9] Nicholas Carlini, Chang Liu, Úlfar Erlingsson, Jernej Kos, and Dawn Song. The secret sharer: Evaluating and testing unintended memorization in neural networks. In *Proceedings of the 28th USENIX Security Symposium, USENIX Security '19*, pp. 267–284, 2019.
- [10] Anne-Sophie Charest. How can we analyze differentially-private synthetic datasets? *Journal of Privacy and Confidentiality*, 2(2):21–33, 2011.
- [11] Kamalika Chaudhuri and Staal A. Vinterbo. A stability-based validation procedure for differentially private machine learning. In *Advances in Neural Information Processing Systems 26, NIPS '13*, pp. 2652–2660. 2013.



- [12] Qingrong Chen, Chong Xiang, Minhui Xue, Bo Li, Nikita Borisov, Dali Kaarfar, and Haojin Zhu. Differentially private data generative models. arXiv preprint 1812.02274, 2018.
- [13] Edward Choi, Siddharth Biswal, Bradley Malin, Jon Duke, Walter F Stewart, and Jimeng Sun. Generating multi-label discrete patient records using generative adversarial networks. In *Proceedings of Machine Learning for Healthcare*, pp. 286–305, 2017.
- [14] Dheeru Dua and Casey Graff. UCI machine learning repository, 2017. URL <http://archive.ics.uci.edu/ml>.
- [15] Cynthia Dwork and Aaron Roth. The algorithmic foundations of differential privacy. *Foundations and Trends in Theoretical Computer Science*, 9(34):211–407, 2014.
- [16] Cynthia Dwork, Frank McSherry, Kobbi Nissim, and Adam Smith. Calibrating noise to sensitivity in private data analysis. In *Proceedings of the 3rd Conference on Theory of Cryptography*, TCC ’06, pp. 265–284, 2006.
- [17] Cynthia Dwork, Guy N. Rothblum, and Salil Vadhan. Boosting and differential privacy. In *Proceedings of the IEEE 51st Annual Symposium on Foundations of Computer Science*, FOCS ’10, pp. 51–60, 2010.
- [18] Lorenzo Frigerio, Anderson Santana de Oliveira, Laurent Gomez, and Patrick Duverger. Differentially private generative adversarial networks for time series, continuous, and discrete open data. In *International Conference on ICT Systems Security and Privacy Protection*, IFIP SEC ’19, pp. 151–164, 2019.
- [19] Marco Gaboardi, Emilio Jesús Gallego Arias, Justin Hsu, Aaron Roth, and Zhiwei Steven Wu. Dual query: Practical private query release for high dimensional data. In *Proceedings of the 31st International Conference on Machine Learning - Volume 32*, ICML’14, pp. 1170–1178, 2014.
- [20] Ian Goodfellow, Jean Pouget-Abadie, Mehdi Mirza, Bing Xu, David Warde-Farley, Sherjil Ozair, Aaron Courville, and Yoshua Bengio. Generative adversarial nets. In *Advances in Neural Information Processing Systems 27*, NIPS ’14, pp. 2672–2680, 2014.
- [21] Google. Tensorflow privacy, 2018. URL <https://github.com/tensorflow/privacy>.
- [22] Ishaan Gulrajani, Faruk Ahmed, Martin Arjovsky, Vincent Dumoulin, and Aaron C. Courville. Improved training of Wasserstein GANs. In *Advances in Neural Information Processing Systems 30*, NIPS ’17, pp. 5767–5777. 2017.
- [23] Anupam Gupta, Katrina Ligett, Frank McSherry, Aaron Roth, and Kunal Talwar. Differentially private combinatorial optimization. In *Proceedings of the 21st annual ACM-SIAM Symposium on Discrete Algorithms*, SODA ’10, pp. 1106–1125, 2010.
- [24] Moritz Hardt and Guy N. Rothblum. A multiplicative weights mechanism for privacy-preserving data analysis. In *Proceedings of the 51st annual IEEE Symposium on Foundations of Computer Science*, FOCS ’10, pp. 61–70, 2010.
- [25] Moritz Hardt, Katrina Ligett, and Frank McSherry. A simple and practical algorithm for differentially private data release. In *Advances in Neural Information Processing Systems 25*, NIPS ’12, pp. 2339–2347. 2012.
- [26] Eric Jang, Shixiang Gu, and Ben Poole. Categorical reparameterization with Gumbel-softmax. arXiv preprint 1611.01144, 2016.
- [27] Alistair E.W. Johnson, Tom J. Pollard, Lu Shen, H. Lehman Li-wei, Mengling Feng, Mohammad Ghassemi, Benjamin Moody, Peter Szolovits, Leo Anthony Celi, and Roger G. Mark. MIMIC-III, a freely accessible critical care database. *Scientific data*, 3:160035, 2016.

- [28] James Jordon, Jinsung Yoon, and Mihaela van der Schaar. PATE-GAN: generating synthetic data with differential privacy guarantees. In *International Conference on Learning Representations, ICLR '19*, 2019. URL <https://openreview.net/forum?id=S1zk9iRqF7>.
- [29] Diederik P. Kingma and Max Welling. Auto-encoding variational bayes. arXiv preprint 1312.6114, 2013.
- [30] Matt J Kusner and José Miguel Hernández-Lobato. GANs for sequences of discrete elements with the Gumbel-softmax distribution. arXiv preprint 1611.04051, 2016.
- [31] Jingcheng Liu and Kunal Talwar. Private selection from private candidates. In *Proceedings of the 51st Annual ACM Symposium on Theory of Computing, STOC '19*, pp. 298–309, 2019.
- [32] H. Brendan McMahan and Galen Andrew. A general approach to adding differential privacy to iterative training procedures. *PPML18: Privacy Preserving Machine Learning - NeurIPS 2018 Workshop*, 2018.
- [33] H. Brendan McMahan, Daniel Ramage, Kunal Talwar, and Li Zhang. Learning differentially private recurrent language models. In *International Conference on Learning Representations, ICLR '17*, 2017. URL <https://openreview.net/forum?id=BJ0hF1Z0b>.
- [34] Ilya Mironov. Rényi differential privacy. In *2017 IEEE 30th Computer Security Foundations Symposium, CSF '17*, pp. 263–275, 2017.
- [35] Mehdi Mirza and Simon Osindero. Conditional generative adversarial nets. arXiv preprint 1411.1784, 2014.
- [36] Olof Mogren. C-RNN-GAN: Continuous recurrent neural networks with adversarial training. *Constructive Machine Learning Workshop (CML) at NeurIPS 2016*, 2016.
- [37] Arvind Narayanan and Vitaly Shmatikov. Robust de-anonymization of large sparse datasets. In *Proceedings of the 2008 IEEE Symposium on Security and Privacy, Oakland S&P '08*, pp. 111–125, 2008.
- [38] NIST. Contest: Nist differential privacy #3. TopCoder, 2019. URL <https://community.topcoder.com/longcontest/?module=ViewProblemStatement&rd=17421&pm=15315>. National Institute of Standards and Technology, Public Safety Communications Research.
- [39] NIST. Differential privacy synthetic data challenge algorithms. NIST Information Technology Laboratory / Applied Cybersecurity Division, 2019. URL <https://www.nist.gov/itl/applied-cybersecurity/privacy-engineering/collaboration-space/browse/de-identification-tools#dpchallenge>. National Institute of Standards and Technology, Privacy Engineering Program.
- [40] Paul Ohm. Broken promises of privacy: Responding to the surprising failure of anonymization. *UCLA Law Review*, 57:1701, 2010.
- [41] Nicolas Papernot, Martín Abadi, Ulfar Erlingsson, Ian Goodfellow, and Kunal Talwar. Semi-supervised knowledge transfer for deep learning from private training data. In *International Conference on Learning Representations, ICLR '17*, 2017. URL <https://openreview.net/forum?id=HkwoSDPgg>.
- [42] Nicolas Papernot, Shuang Song, Ilya Mironov, Ananth Raghunathan, Kunal Talwar, and Úlfar Erlingsson. Scalable private learning with PATE. In *International Conference on Learning Representations, ICLR '18*, 2018. URL <https://openreview.net/forum?id=rkZB1XbRZ>.
- [43] Mijung Park, James Foulds, Kamalika Choudhary, and Max Welling. DP-EM: Differentially Private Expectation Maximization. In *Proceedings of the 20th International Conference on Artificial Intelligence and Statistics, AISTATS '17*, pp. 896–904, 2017.

- [44] Haoyue Ping, Julia Stoyanovich, and Bill Howe. DataSynthesizer: Privacy-preserving synthetic datasets. In *Proceedings of the 29th International Conference on Scientific and Statistical Database Management, SSDBM '17*, pp. 42:1–42:5, 2017.
- [45] Masaki Saito, Eiichi Matsumoto, and Shunta Saito. Temporal generative adversarial nets with singular value clipping. In *Proceedings of the IEEE International Conference on Computer Vision, ICCV '17*, pp. 2830–2839, 2017.
- [46] Tim Salimans, Ian Goodfellow, Wojciech Zaremba, Vicki Cheung, Alec Radford, and Xi Chen. Improved techniques for training GANs. In *Advances in Neural Information Processing Systems 29, NIPS '16*, pp. 2234–2242. 2016.
- [47] H. Surendra and H.S. Mohan. A review of synthetic data generation methods for privacy preserving data publishing. *International Journal of Scientific and Technology*, 6:95–101, 2017.
- [48] Om Thakkar, Galen Andrew, and H. Brendan McMahan. Differentially private learning with adaptive clipping. arXiv preprint 1905.03871, 2019.
- [49] Reihaneh Torkzadehmahani, Peter Kairouz, and Benedict Paten. DP-CGAN: Differentially private synthetic data and label generation. In *Proceedings of the IEEE Conference on Computer Vision and Pattern Recognition (CVPR) Workshops*, 2019.
- [50] Aleksei Triastcyn and Boi Faltings. Generating artificial data for private deep learning. arXiv preprint 1803.03148, 2018.
- [51] Koen Lennart van der Veen, Ruben Seggers, Peter Bloem, and Giorgio Patrini. Three tools for practical differential privacy. *PPML18: Privacy Preserving Machine Learning - NeurIPS 2018 Workshop*, 2018.
- [52] Tim Van Erven and Peter Harremo. Rényi divergence and Kullback-Leibler divergence. *IEEE Transactions on Information Theory*, 60(7):3797–3820, 2014.
- [53] Hongwei Wang, Jia Wang, Jialin Wang, Miao Zhao, Weinan Zhang, Fuzheng Zhang, Xing Xie, and Minyi Guo. GraphGAN: Graph representation learning with generative adversarial nets. In *Proceedings of the 32nd AAAI Conference on Artificial Intelligence, AAAI '18*, pp. 2508–2515, 2018.
- [54] Yu-Xiang Wang, Borja Balle, and Shiva Kasiviswanathan. Subsampled rényi differential privacy and analytical moments accountant. In *Proceedings of the 22th International Conference on Artificial Intelligence and Statistics, AISTATS '19*, pp. 1226–1235, 2019.
- [55] Liyang Xie, Kaixiang Lin, Shu Wang, Fei Wang, and Jiayu Zhou. Differentially private generative adversarial network. arXiv preprint 1802.06739, 2018.
- [56] Lei Yu, Ling Liu, Calton Pu, Mehmet Emre Gursoy, and Stacey Truex. Differentially private model publishing for deep learning. In *Proceedings of the 40th IEEE Symposium on Security and Privacy, Oakland S&P '19*, pp. 326–343, 2019.
- [57] Jun Zhang, Graham Cormode, Cecilia M Procopiuc, Divesh Srivastava, and Xiaokui Xiao. PrivBayes: Private data release via Bayesian networks. *ACM Transactions on Database Systems (TODS)*, 42(4): 25, 2017.
- [58] Xinyang Zhang, Shouling Ji, and Ting Wang. Differentially private releasing via deep generative model (technical report). arXiv preprint 1801.01594, 2018.

## A Algorithm Description and Pseudocode of DP-Auto-GAN

In this appendix, we provide the pseudocode of the subroutines in DP-auto-GAN (Algorithm 2):  $\text{DPTRAIN}_{\text{AUTO}}$ ,  $\text{DPTRAIN}_{\text{DISCRIMINATOR}}$ , and  $\text{TRAIN}_{\text{GENERATOR}}$ . The complete DP-auto-GAN algorithm is specified by the architecture and training parameters of the encoder, decoder, generator, and discriminator.

After initial data pre-processing, the  $\text{DPTRAIN}_{\text{AUTO}}$  algorithm trains the autoencoder. Details of this training process are fully specified in Algorithm 3. As noted earlier, the decoder is trained privately by clipping gradient norm and injecting Gaussian noise in order to obtain the gradient of decoder  $g_\theta$ , while the gradient of encoder  $g_\phi$  can be used directly as encoder can be trained non-privately.

The second phase of DP-auto-GAN is to train the GAN. As suggested by [20], the discriminator trained for several iterations per one iteration of generator training. While the discriminator is being trained, the generator is fixed, and vice-versa. The discriminator and generator training are described in Algorithms 4 ( $\text{DPTRAIN}_{\text{DISCRIMINATOR}}$ ) and 5 ( $\text{TRAIN}_{\text{GENERATOR}}$ ) respectively. Since the discriminator receives real data samples as input for training, the training is made differentially private by clipping the norm of the gradient updates, and adding Gaussian noise to the gradient  $g$ . The generator does not use any real data in training (or any functions of the real data that were computed without differential privacy), and hence it can be trained without any need to clip the gradient norm or to inject noise into the gradient.

Finally, the overall privacy analysis of DP-auto-GAN is done via the RDP accountant for each training, and composing at the RDP level (as a function of  $\alpha$ ) as described in Corollary 4. After the sum of the RDP privacy parameters is obtained (which is a function of  $\alpha$ ), then for any given fixed  $\delta$ , we optimize  $\alpha$  to get the best  $\epsilon$  in Proposition 3. Because the value of  $\epsilon(\alpha)$  obtained from Proposition 3 is a convex function of  $\alpha$  [52, 54], we implement ternary search to efficiently optimize for  $\alpha$ .

**Proposition 5.** *DP-auto-GAN trained with differentially private algorithms  $\mathcal{M}_1$  on the decoder and  $\mathcal{M}_2$  on the discriminator (and possibly a non-private algorithm on the encoder) achieves differential privacy guarantee equivalent to that of the composition of  $\mathcal{M}_1, \mathcal{M}_2$ .*

*Proof.* DP-auto-GAN needs to release only generator and decoder as an output. Releasing the decoder incurs cost of privacy equal to that of  $\mathcal{M}_1$ . The generator accesses the data only through a discriminator, which is differentially private by mechanism  $\mathcal{M}_2$ , so releasing the generator has the same privacy loss as  $\mathcal{M}_2$  from post-processing. Therefore, releasing both decoder and generator incurs privacy loss of composition of  $\mathcal{M}_1$  and  $\mathcal{M}_2$ .  $\square$

Proposition 5 is stated more formally using the RDP notion of privacy (where the privacy parameters are a function of  $\alpha$ ) in Corollary 4 in the main body. That corollary follows immediately from Propositions 5 and 2.

## B Additional Experimental Details

### B.1 Model and Training Specification of Experiment on MIMIC-III data

The autoencoder was trained via Adam with Beta 1 = 0.9, Beta 2 = 0.999, and a learning rate of 0.001. It was trained on minibatches of size 100 and microbatches of size 1. L2 clipping norm was selected to be the median L2 norm observed in a non-private training loop, set to 0.8157. The noise multiplier was then calibrated to achieve the desired privacy guarantee.

The GAN was composed of two neural networks, the generator and the discriminator. The generator was a simple feed-forward neural network, trained via RMSProp with alpha = 0.99 with a learning rate of 0.001. The discriminator was also a simple feed-forward neural network, also trained via RMSProp with the same parameters. The L2 clipping norm of the discriminator was set to 0.35. The pair was trained on minibatches of size 1,000 and a microbatch size of 1, with 2 updates to the discriminator per 1 update to the generator. Again, the noise multiplier was then calibrated to achieve desired privacy guarantees.

A serialization of the model architectures used in the experiment can be found below.

---

**Algorithm 3** DPTRAIN<sub>AUTO</sub>( $X, En_\phi, De_\theta$ , training parameters)

---

- 1: **training parameter input:** Learning rate  $\eta_1$ , number of iteration rounds (or optimization steps)  $T_1$ , loss function  $L_{\text{auto}}$ , optimization method OPTIM<sub>auto</sub> batch sampling rate  $q_1$  (for the batch expectation size  $b_1 = q_1 m$ ), clipping norm  $C_1$ , noise multiplier  $\psi_1$ , microbatch size  $r_1$
  - 2: **goal:** train one step of autoencoder ( $En_\phi, De_\theta$ )
  - 3: **procedure** DPTRAIN<sub>AUTO</sub>
  - 4:    $\mathcal{B} \leftarrow \text{SAMPLEBATCH}(X, q_1)$
  - 5:   Partition  $\mathcal{B}$  into  $B_1, \dots, B_k$  each of size  $r$  (ignoring the dividend)
  - 6:    $\hat{k} \leftarrow \frac{q_1 m}{r}$   $\triangleright$  an estimate of  $k$
  - 7:   **for**  $j = 1 \dots k$  **do**
  - 8:      $\triangleright$  Both  $g_\phi^j, g_\theta^j$  can be computed in one backpropagation
  - 9:      $g_\phi^j, g_\theta^j \leftarrow \nabla_\phi(L_{\text{auto}}(De_\theta(En_\phi(B_j)), B_j)), \nabla_\theta(L_{\text{auto}}(De_\theta(En_\phi(B_j)), B_j))$
  - 10:     $g_\phi \leftarrow \frac{1}{k} \sum_{j=1}^k g_\phi^j$
  - 11:     $g_\theta \leftarrow \frac{1}{k} \left( \left( \sum_{j=1}^k \text{CLIP}(g_\theta^j, C_1) \right) + \mathcal{N}(0, C_1^2 \psi_1^2 I) \right)$
  - 12:     $(\phi, \theta) \leftarrow \text{OPTIM}_{\text{auto}}(\phi, \theta, g_\phi, g_\theta, \eta_1)$
- 

---

**Algorithm 4** DPTRAIN<sub>DISCRIMINATOR</sub>( $X, Z, G_w, De_\theta, D_y$ , training parameters)

---

- 1: **training parameter input:** Learning rate  $\eta_3$ , number of discriminator iterations per generator step  $t_D$ , loss function  $L_D$ , optimization method OPTIM<sub>D</sub>, batch sampling rate  $q_3$  (for the batch expectation size  $b_3 = q_3 m$ ), clipping norm  $C_3$ , noise multiplier  $\psi_3$ , microbatch size  $r_3$
- 2: **goal:** train one step of discriminator  $D_y$
- 3: **procedure** DPTRAIN<sub>DISCRIMINATOR</sub>
- 4:    $\mathcal{B} \leftarrow \text{SAMPLEBATCH}(X, q_3)$
- 5:   Partition  $\mathcal{B}$  into  $B_1, \dots, B_k$  each of size  $r$  (ignoring the dividend)
- 6:    $\hat{k} \leftarrow \frac{q_3 m}{r}$   $\triangleright$  an estimate of  $k$
- 7:   **for**  $j = 1 \dots k$  **do**
- 8:      $\{z_i\}_{i=1}^r \sim Z^r$
- 9:      $B' \leftarrow \{De(G_w(z_i))\}_{i=1}^r$
- 10:     $g^j \leftarrow \nabla_y(L_D(B_j, B', D_y))$
- 11:     $\triangleright$  In the case of WGAN,

$$L_D(B_j, B', D_y) := \frac{1}{r} \sum_{b \in B_j} D_y(b) - \frac{1}{r} \sum_{b' \in B'} D_y(b')$$

- 11:     $g \leftarrow \frac{1}{k} \left( \left( \sum_{j=1}^k \text{CLIP}(g^j, C_3) \right) + \mathcal{N}(0, C_3^2 \psi_3^2 I) \right)$
  - 12:     $y \leftarrow \text{OPTIM}_D(y, g, \eta_3)$
-

---

**Algorithm 5** TRAIN<sub>GENERATOR</sub>( $Z, G_w, De_\theta, D_y$ , generator training parameters)

---

- 1: **training parameter input:** Learning rate  $\eta_2$ , batch size  $b_2$ , loss function  $L_G$ , optimization method  $\text{OPTIM}_G$ , number of generator iteration rounds (or optimization steps)  $T_2$
- 2: **goal:** train one step of generator  $G_w$
- 3: **procedure** TRAIN<sub>GENERATOR</sub>
- 4:    $\{z_i\}_{i=1}^{b_2} \sim Z^{b_2}$
- 5:    $B' \leftarrow \{De(G_w(z_i))\}_{i=1}^{b_2}$
- 6:    $g \leftarrow \nabla_w(L_G(B', D_y))$   
    ▷ In the case of WGAN,

$$L_G(B', D_y) := -\frac{1}{b_2} \sum_{b' \in B'} D_y(b')$$

- 7:    $w \leftarrow \text{OPTIM}_G(w, g, \eta_2)$
- 

```
(encoder): Sequential(
(0): Linear(in-feature=1071, out-feature=128, bias=True)
(1): Tanh()
)
(decoder): Sequential(
(0): Linear(in-feature=128, out-feature=1071, bias=True)
(1): Sigmoid()
)

Generator(
(model): Sequential(
(0): Linear(in-feature=128, out-feature=128)
(1): LeakyReLU(negative-slope=0.2)
(2): Linear(in-feature=128, out-feature=128)
(3): Tanh()
)
)

Discriminator(
(model): Sequential(
(0): Linear(in-feature=1071, out-feature=256, bias=True)
(1): LeakyReLU(negative-slope=0.2)
(2): Linear(in-feature=256, out-feature=1, bias=True)
)
)
```

## B.2 Additional MIMIC-III Empirical Results

Here show Figure 7, which is the full version of Figure 3 (dimension-wise prediction for MIMIC-III dataset), before cleaning the data by removing features with sparse values of 1. As observed in the figure, smaller  $\epsilon$  values cause more features the in synthetic data to have a high proportion of 0's so the logistic regression classifier trained on these features uniformly outputs 0, causing a default AUROC score of 1/2. A closer inspection of real data shows that nearly all of those features indeed have very sparse 1's (appearing less than 1% of the time). This suggests that with smaller  $\epsilon$  values, the features that always output as 0 have been learned accurately with respect to the training set, but may not necessarily generalize to the hold-out test set.

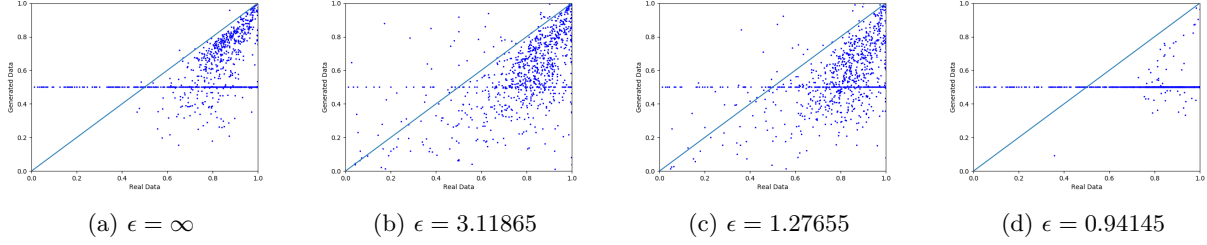


Figure 7: Full plots of dimension-wise prediction for MIMIC-III dataset

### B.3 Model and Training Specification of Experiment on ADULT data

The autoencoder was trained via Adam with Beta 1 = 0.9, Beta 2 = 0.999, and a learning rate of 0.005 for 20,000 minibatches of size 64 and a microbatch size of 1. The L2 clipping norm was selected to be the median L2 norm observed in a non-private training loop, equal to 0.012. The noise multiplier was then calibrated to achieve the desired privacy guarantee.

The GAN was composed of two neural networks, the generator and the discriminator. The generator used a ResNet architecture, adding the output of each block to the output of the following block. It was trained via RMSProp with alpha = 0.99 with a learning rate of 0.005. The discriminator was a simple feed-forward neural network with LeakyReLU hidden activation functions, also trained via RMSProp with alpha = 0.99. The L2 clipping norm of the discriminator was set to 0.022. The pair was trained on 15,000 minibatches of size 128 and a microbatch size of 1, with 15 updates to the discriminator per 1 update to the generator. Again, the noise multiplier was then calibrated to achieve the desired privacy guarantee.

A serialization of the model architectures used in the experiment can be found below.

```

Autoencoder(
(encoder): Sequential(
0: Linear(in-features=106, out-feature=60, bias=True)
(1): LeakyReLU(negative-slope=0.2)
(2): Linear(in-feature=60, out-feature=15, bias=True)
(3): LeakyReLU(negative-slope=0.2)
)
(decoder): Sequential(
(0): Linear(in-feature=15, out-feature=60, bias=True)
(1): LeakyReLU(negative-slope=0.2)
(2): Linear(in-feature=60, out-feature=106, bias=True)
(3): Sigmoid()
)
)
Generator(
(block-0): Sequential(
(0): Linear(in-feature=64, out-feature=64, bias=False)
(1): BatchNorm1d()
(2): LeakyReLU(negative-slope=0.2)
)
(block-1): Sequential(
(0): Linear(in-feature=64, out-feature=64, bias=False)
(1): BatchNorm1d()
(2): LeakyReLU(negative-slope=0.2)
)
(block-2): Sequential(

```

```

(0): Linear(in-feature=64, out-feature=15, bias=False)
(1): BatchNorm1d()
(2): LeakyReLU(negative-slope=0.2)
)
)
    Discriminator(
(model): Sequential(
(0): Linear(in-feature=106, out-feature=70, bias=True)
(1): LeakyReLU(negative-slope=0.2)
(2): Linear(in-feature=70, out-feature=35, bias=True)
(3): LeakyReLU(negative-slope=0.2)
(4): Linear(in-feature=35, out-feature=1, bias=True) )
)

```

## C Additional Related Work

### C.1 Differentially Private Training of Deep Models

There are numerous works on optimizing the performance of differentially private GANs, including data partitioning (either by class of labels in supervised setting or a private algorithm) [56, 41, 42, 28, 2, 3, 12]; reducing the number of parameters in deep models [33]; changing the norm clipping for the gradient in DP-SGD during training [33, 51, 48]; changing parameters of the Gaussian noise used during training [56]; and using publicly available data to pre-train the private model with a warm start [58, 33]. Clipping gradients per-layer of models [32, 33] and per-dynamic parameter grouping [58] are also proposed. Additional details for some of these optimization approaches are given below.

**Batch Sampling** Three ways are known to sample a batch from data in each optimization step. These methods are described in [32]; we summarize them here for completeness. The first is to sample each individual’s data independently with a fixed probability. This sampling procedure is the one used in the analysis of the subsampled moment accountant in [1, 32] and subsampled RDP composition in [34]. This RDP composition is publicly available at Tensorflow Privacy [21]. We implement this sampling procedure and use Tensorflow Privacy to account Renyi Divergence during training. Another sampling policy is to sample uniformly at random a fixed-size subset of all datapoints. This achieves a different RDP guarantee, which was analyzed in [54]. Finally, a common subsampling procedure is to shuffle the data via uniformly random permutation, and take a fixed-size batch of the first  $k$  points in shuffled order. The process is repeated after a pass over all datapoints (an epoch). Although this batch sampling is most common in practice, no subsampled privacy composition is known in this case for the centralized model.

**Hyperparameter Tuning** Training deep learning models involves hyperparameter tuning to find good architecture and optimization parameters. This process is also done differentially privately, and the privacy budget must be accounted for. Abadi et al. [1] accounts for hyperparameter search using the work of [23]. Beaulieu-Jones et al. [7] uses Report Noisy Max [15] to private select a model with top performance when a model evaluation metric is known. Some work has also been done to account for selecting high-performance models without spending much privacy budget [11, 31]. In our experimental work, we omit the privacy accounting of hyperparameter search, as this is not the focus of our contribution.

### C.2 Evaluation Metrics for Synthetic Data

In this section, we review the evaluation schemes for measuring quality of synthetic data and discuss our contribution of novel metrics in comparison with existing literature. Various evaluation metrics have been considered in the literature to quantify the quality of synthetic data [10]. Broadly, evaluation metrics can



be divided into two major categories: supervised and unsupervised. Supervised evaluation metrics are used when clear distinctions exist between features and labels in the dataset, e.g., for healthcare applications, whether a person has a disease or not could be a natural label. Unsupervised evaluation metrics are used when no feature of the data can be decisively termed as a label. For example, a data analyst who wants to learn a pattern from synthetic data may not know what specific prediction tasks to perform, but rather wants to explore the data using an unsupervised algorithm such as Principle Component Analysis (PCA). Unsupervised metrics can then be divided into three broad types: prediction-based, distributional-distance-based, and qualitative (or visualization-based). We describe supervised evaluation metrics and all three types of unsupervised evaluation metrics below. Metrics in previous work and our proposed metrics are summarized in Table 2 in Section 4.

**Supervised evaluation metrics.** The main aim of generating synthetic data in a supervised setting is to best understand the relationship between features and labels. A popular metric for such cases is to train a machine learning model on the synthetic data and report its accuracy on the real test data [55]. Zhang et al. [58] used inception scores on the image data with classification tasks. Inception scores were proposed in Salimans et al. [46] for images which measure quality as well as diversity of the generated samples. Another metric used in Jordon et al. [28] reports whether the accuracy ranking of different machine learning models trained on the real data is preserved when the same machine learning model is trained on the synthetic data. Although these metrics are used for classification in the literature, they can be easily generalized to the regression setting.

**Unsupervised evaluation metric, prediction-based.** Rather than measuring accuracy by predicting one particular feature as in supervised-setting, one can predict *every* individual feature using the rest of features. The prediction score is therefore created for each single feature, creating a list of dimension- (or feature-) wise prediction scores. Good synthetic data should have similar dimension-wise prediction scores to that of the real data. Intuitively, similar dimension-wise prediction shows that synthetic data correctly captures inter-feature relationships in the real data.

One metric of this type is proposed by Choi et al. [13] for binary data. Although it was originally proposed for binary data, we extend this to mixed-type data by allowing varieties of predictive models appropriate for each data type present in the dataset. For each feature, we try predictive models on the real dataset in order of increasing complexity until a good accuracy score is achieved. For example, to predict a real-valued feature, we first used a linear classifier and then a neural network predictor. This ensures that a choice of predictive model is appropriate to the feature. Synthetic data is then evaluated by measuring the accuracy of the same predictive model (trained on the real data) on the synthetic data. Similarly high accuracy scores on synthetic data and real data indicates that the synthetic data closely approximates the real data.

Zhang et al. [58] provides an unsupervised Jensen-Shannon score metric which measures the Jensen-Shannon divergence between the output of a discriminating neural network on the real and synthetic datasets, and a Bernoulli random variable with 0.5 probability. This metric differs from dimension-wise prediction in that the predictive model (discriminator) is trained over the whole dataset at once, rather than dimension-wise, to obtain a score.

**Unsupervised evaluation metric, distributional-distance-based.** Another way to evaluate the quality of synthetic data is computing a dimension-wise probability distribution, which was also proposed in Choi et al. [13] for binary data. This metric compares the marginal distribution of real and synthetic data on each individual feature. Below we survey other metrics in this class that can extend to mixed-type data.

*3-way marginal:* Recently, the NIST [38] challenge used a 3-way marginal evaluation metric in which three random features of the real and synthetic data  $R, S$  are used to compute the total variation distance as a statistical score. This process is repeated a few times and finally, average score is returned. In particular, values for each of the three features are partitioned in 100 disjoint bins as follows:

$$B_{R,k}^i = \left\lfloor \frac{(R_k^i - R_{k,\min}) * 100}{R_{k,\max} - R_{k,\min}} \right\rfloor \text{ and } B_{S,k}^i = \left\lfloor \frac{(S_k^i - R_{k,\min}) * 100}{R_{k,\max} - R_{k,\min}} \right\rfloor,$$

where  $R_k^i, S_k^i$  is the value of  $i$ -th datapoint's  $k$ -th feature in datasets  $R$  and  $S$ , and  $R_{k,\min}, R_{k,\max}$  are respectively the minimum and maximum value of the  $k$ -th feature in  $R$ . For example, if  $k = 1, 2, 3$  are the selected features then  $i$ -th data points of  $R$  and  $S$  are put into bins identified by a 3-tuple,  $(B_{R,1}^i, B_{R,2}^i, B_{R,3}^i)$  and  $(B_{S,1}^i, B_{S,2}^i, B_{S,3}^i)$ , respectively.

Let  $\mathcal{B}_R, \mathcal{B}_S$  be the set of all 3-tuple bins in datasets  $R$  and  $S$ , and let  $|B|$  denote number of datapoints in 3-tuple bin  $B$ , normalized by total number of data points. Then, the 3-way marginal metric reports the  $\ell_1$ -norm of the bin-wise difference of  $\mathcal{B}_R$  and  $\mathcal{B}_S$  as follows:

$$\sum_{B_1 \in \mathcal{B}_R} \sum_{B_2 \in \mathcal{B}_S} \mathbb{I}_{\{B_1 \in \mathcal{B}_S\}} \mathbb{I}_{\{B_2 = B_1\}} ||B_1| - |B_2|| + \sum_{B_1 \in \mathcal{B}_R} (1 - \mathbb{I}_{\{B_1 \in \mathcal{B}_S\}}) |B_1| + \sum_{B_2 \in \mathcal{B}_S} (1 - \mathbb{I}_{\{B_2 \in \mathcal{B}_R\}}) |B_2|.$$

Both aforementioned metrics (dimension-wise probability from [13] and 3-way marginal from [38]) involve two steps. First, a projection (or a selection of features) of data is specified, and second some statistical distance or visualization of synthetic and real data in the projected space is computed. Dimension-wise probability for binary data corresponds to projecting data into each single dimension, and visualizing synthetic and real distributions in projected space by histograms (for binary data, the histogram can be specified by one single number: probability of the feature being 1). The 3-way marginal metric first selects a three-dimensional space specified by three features as a space into which data projected, discretizes the synthetic and real distributions on that space, then computes a total variation distance between discretized distributions. Our proposed metrics generalize both steps of designing the metric as follows.

*Generalization of Data Projection:* One can generalize selection of 3 features (3-way marginal) to any  $k$  features ( $k$ -way marginal). However, one can also select  $k$  *principle components* instead of  $k$  features. We distinguish these as  $k$ -way *feature* marginal (projection onto a space spanned by feature dimensions) and  $k$ -way *PCA* marginal (projection onto a space spanned by principle components of the original dataset). Intuitively,  $k$ -way PCA marginal best compresses the information of the real data into a small  $k$ -dimensional space, and hence is a better candidate for comparing projected distributions.

*Generalization of Distributional Distance:* Total variation distance can be misleading as it does not encode any information on the distance between the supports of two distributions. In general, one can define any metric of choice (optionally with discretization) on two projected distributions, such as Wasserstein distance which also depends on the distance between the supports of the two distributions.

*Distributional Distance:* The distance between two distributions can also be computed without any data projections. Computing an exact statistical score on high-dimensional datasets is likely computationally hard. However, we can subsample uniformly at random points from two distributions to compute the score more efficiently, then average this distance over many iterations.

**Unsupervised evaluation metric, qualitative.** As described above, dimension-wise probability is a specific application of comparing histograms under binary data. One can plot histograms of each feature (1-way feature marginal) for inspection. In practice, histogram visualization is particularly helpful when a feature is strongly skewed, sparse (majority zero), and/or hard to predict well by predictive models. An example of this occurred when predictive models do not have meaningful predictive accuracy on certain features of the ADULT dataset, making prediction-based metric inappropriate. Instead inspection of histograms of those features on synthetic and real data (as in Figure 6) indicate that synthetic data replicates those features well.

In addition, 2-way PCA marginal is a visual representation of data that explains as much variance as possible in a plane, providing a good trade-off between information and ease of visualization on two datasets. This visualization can be augmented with a distributional distance of choice over the two distributions on these two spaces to get a quantitative metric.